Electrochemical access to functionalized dihydrothiopyran derivatives. Part 1: Electroreduction of tetraactivated 4*H*-thiopyrans

D. Rondeau,[a] E. Raoult,[a] A. Tallec,[a] S. Sinbandhit,[b] L. Toupet,[c] A. Imberty[d] and J. P. Pradère*,[d]

[a] *Laboratoire d'Electrochimie—URA au CNRS No. 439.*
[b] *Centre Régional de Mesures Physiques de l'Ouest.*
[c] *Groupe Matière condensée et Matériaux, URA au CNRS No. 804 Université de Rennes 1 —Campus de Beaulieu—35042 Rennes Cédex, France.*
[d] *Laboratoire de Synthèse Organique—URA au CNRS No. 475 2, rue de la Houssinière—44072 Nantes Cédex, 03 France*

Electroreduction of tetraactivated 4*H*-thiopyrans leads selectively to diastereoisomers of dihydrothiopyrans. The relative percentages depend on the experimental conditions (electrolysis in sulfuric medium, ammoniacal buffer). The preferred conformations of the end-products are determined in solid state by X-ray crystallography and in solution by ^{1}H NMR spectroscopy, then compared with molecular modelling results. The relative conformations of the diastereoisomers and their ratio are established by ^{1}H NMR spectroscopy.

Introduction

The use of electrochemistry as a powerful tool for the reduction of heterocycles containing sulfur and nitrogen atoms has been widely demonstrated.[1] In particular, controlled potential electrolysis of activated 4*H*-1,3-thiazines **A** leads to 6*H*-1,3-thiazine or pyrrole derivatives. There appears to be a strong correlation between the nature of the isolated products and the pH of the medium.[2] A theoretical approach was used to determine the influence of the nitrogen atom in the thiazine ring on the chemoselectivity of the electroreduction.[3] Consequently, we became interested in comparing the evolution of activated 4*H*-thiopyran derivatives **B** in electrolytic media with that for the **A** derivative.

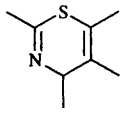

A

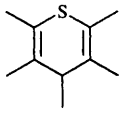

B

We now propose an electrochemical route to prepare functionalized dihydrothiopyrans from 4*H*-thiopyran precursors. Substituted dihydrothiopyran derivatives, considered as useful synthetic intermediates,[4] can generally be obtained by the dimerization of thiochalcones generated *in situ*[5–7] or by a cycloaddition from stabilized α,β-unsaturated thiones and activated dienophiles.[8–10] In these cases an elimination reaction may occur leading to activated 2*H*-thiopyrans.[11] Dihydrothiopyrans may also be obtained by cycloaddition from activated thiones as heterodienophile.[12]

The methodology developed in our work presents two key steps. First a hetero-Diels–Alder reaction from functionalized thioamide vinylogue generates activated 4*H*-thiopyrans **B** substituted at position 4 by an electron releasing group. The second step involves the electroreduction of isolated unsaturated cycloadducts **B** leading selectively to dihydrothiopyran derivatives **C**. This allows a detailed study of the stereochemistry of the reduction.[13]

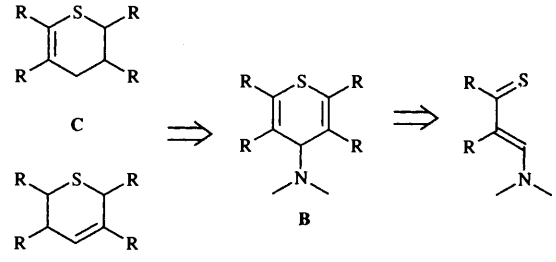

R = electron-withdrawing group

Results

Synthesis of 4-dimethylamino-2,3,5,6-tetramethoxycarbonyl-4*H*-thiopyran

Access to tetrafunctionalized 4*H*-thiopyrans was easily obtained from the N^1-thioacylamidine **1** by using a cycloaddition–cycloreversion process described in the literature.[14] A cycloaddition reaction of heterodienic compound **1** and dimethyl acetylenedicarboxylate (DMAD), was followed by thermolysis of the corresponding 4*H*-1,3-thiazine cycloadduct giving the functionalized thioamide vinylogue **2**. Further cycloaddition reaction of **2** with DMAD led to the tetrasubstituted 4*H*-thiopyran **3** (Scheme 1). The 4*H*-thiopyran **3** can also be synthesized directly from the N^1-thioacylamidine **1** by treatment with an excess of DMAD.

Electrochemical investigations

The electrochemical behaviour of the tetrasubstituted thiopyran **3** has been investigated in aqueous-alcoholic mixtures.

(*i*) Whatever the acidity of the supporting electrolyte, an irreversible four-electron reduction is observed; some half-wave potentials, measured in equal volume mixtures of aqueous supporting electrolyte and ethanol are given in Table 1.

A more complete study, carried out in Britton–Robinson buffers (Fig. 1), shows that in acidic medium, $E_{1/2}$ depends on the medium acidity according to eqn. (1). Then, protonation of the amino group takes place before electron-transfer.

Table 1 Half-wave potentials of compound **3**[a]

Aqueous supporting electrolyte	$E_{1/2}$/V *vs.* SCE
Sulfuric acid (0.5 mol l^{-1})	−0.47
Acetic buffer (0.5 mol l^{-1})	−0.66
Ammoniacal buffer (0.5 mol l^{-1})	−0.87

[a] Substrate concentration: 10^{-3} mol l^{-1}; dropping time $\tau = 2$ s.

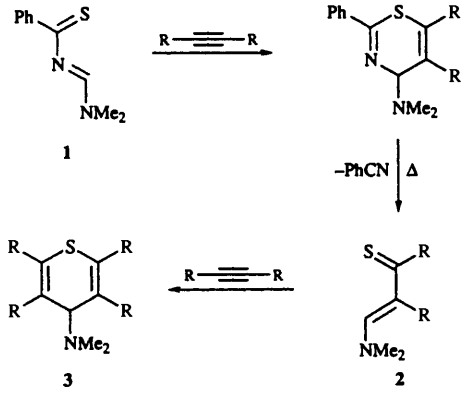

Scheme 1 R = CO_2Me

$$E_{1/2}(\text{V } vs. \text{ SCE}) = -0.45\text{–}0.05\ \text{pH} \qquad (1)$$

In a basic medium, $E_{1/2}$ is constant (−1.06 V *vs.* SCE) and direct reduction of the neutral molecule occurs. Moreover, between pH 6 and 7, a superposition of two polarographic waves occurs corresponding to the two processes previously described. The determination of the half-wave potentials is not possible.

(*ii*) Macroscale electroreductions were carried out at constant potential, in a mixture of aqueous electrolyte and ethanol (1:2), in very acidic (sulfuric acid 0.5 mol l^{-1}, E = −0.7 V *vs.* SCE) or basic (ammoniacal buffer 0.5 mol l^{-1}, E = −1.3 V *vs.* SCE) media. The electricity consumption, measured by coulometry, is four-electron mol per mol of substrate. Work-up of the solution (see Experimental part) leads to a mixture of four 5,6-dihydro-2*H*-thiopyran diastereoisomers **4a–d** (Scheme 2), analysed by NMR spectroscopy.

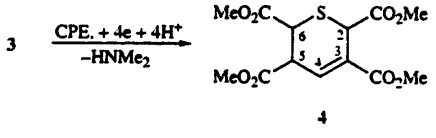

Scheme 2 CPE = Controlled potential electrolysis

The reduction of the ethylenic double bond and the loss of dimethylamine are confirmed by spectral and elemental analysis of the resulting tetramethoxycarbonyl-5,6-dihydro-2*H*-thiopyrans, **4**. The ^{13}C NMR spectra show the presence of four diastereoisomers **4a–d**. The ratio of these diastereoisomers seems to depend on the electrolytic medium, and can be determined by ^1H NMR spectroscopy using the chemical shift difference of the proton H-4. We wanted to determine their relative configurations, and they were separated by liquid chromatography to obtain two pairs of diastereoisomers initially, which served three purposes.

(*i*) To assign the ^1H NMR signals for each proton of the dihydrothiopyran ring.

(*ii*) To establish the predominant or preferred ring conformation in solution in order to predict the dihedral angles of the molecule and to detect homonuclear interaction in ^1H NMR.

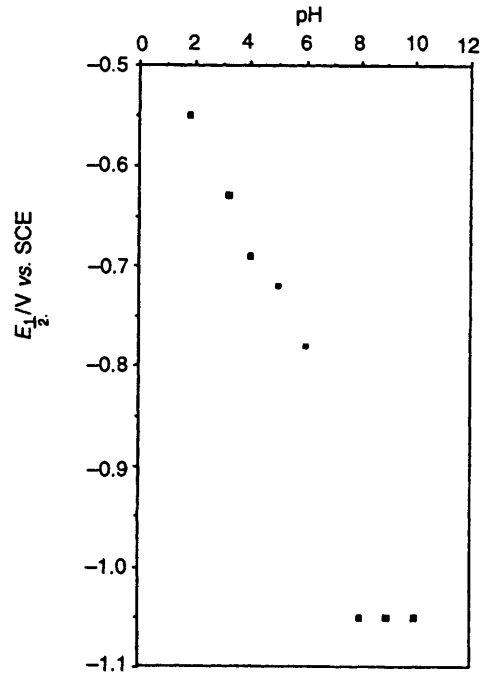

Fig. 1 Relationship between the pH and the half-wave potential of reduction of 4*H*-thiopyran **3** in Britton–Robinson buffer. Conditions as in Table 1.

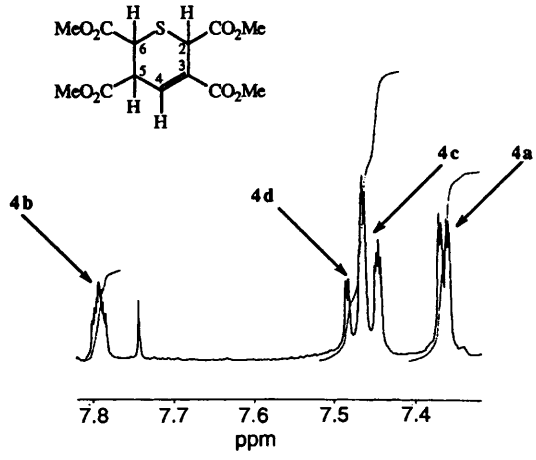

Fig 2 ^1H NMR signal of the proton in position 4 for all diastereoisomers **4a–d** (spectrum recorded after electrolysis in a basic medium)

(*iii*) To identify each diastereoisomer by assigning the axial or equatorial position of the ring-protons using the correlations between the dihedral angles and the coupling constants.

In a second step, this approach allows a quantitative determination of the 5,6-dihydro-2*H*-thiopyrans in the electrolysis solution, thus avoiding any epimerization during treatment.

^1H NMR spectroscopy of the 2,3,5,6-tetramethoxycarbonyl-5,6-dihydro-2*H*-thiopyrans 4a–d

In order to maintain a rigorous and identical approach in deducing the structures of each 5,6-dihydro-2*H*-thiopyran, the vinylic proton 4-H was used (Fig. 2). This proton is easily identified due to its low-field chemical shift, and serves as a convenient starting point for tracing the 2-H, 5-H and 6-H coupling network in the thiopyran ring by homonuclear experiments. ^1H NMR signals are then assigned to 2-H, 5-H and 6-H for each diastereoisomer **4a–d**. Coupling constants and chemical shifts of the protons in compounds **4a–d** are listed in Table 2.

Table 2 ^{1}H NMR data of the 2,3,5,6-tetramethoxycarbonyl-5,6-dihydro-2*H*-thiopyrans

	4a	4b	4c	4d
$\delta(CDCl_3)^a$	4.3	4.3	4.2 to 4.3[c]	4.26
2-H (multiplicity)	(m)	(t)	(t)	(t)
$\delta(C_6D_6)^a$	4.29	4.33	4.2	4.23
$\delta(CDCl_3)^a$	7.36	7.48	7.45	7.79
4-H (multiplicity)	(dt)	(dd)	(ddd)	(dddd)
$\delta(C_6D_6)^a$	7.45	7.48	7.49	7.9
$\delta(CDCl_3)^a$	3.98	3.7 to 3.9	4.21 to 4.3[c]	3.7 to 3.9[c]
5-H (multiplicity)	(dt)	(ddd)	(dd)	(m)
$\delta(C_6D_6)^a$	4.11	3.79	4.1	3.07
$\delta(CDCl_3)^a$	4.3	4.27	4.2 to 4.3[c]	4.1
6-H (multiplicity)	(d)	(d)	(d)	(dd)
$\delta(C_6D_6)^a$	4.7	4.38	4.18	3.76
$\delta(CDCl_3)^a$	3.7 to 3.9	3.7 to 3.9	3.7 to 3.9	3.7 to 3.9
CO_2CH_3	(s)	(s)	(s)	(s)
$\delta(C_6D_6)^a$	3.1 to 3.4	3.1 to 3.4	3.1 to 3.4	3.1 to 3.4
$J_{24}{}^b$	0.9	1	1	1.9
$J_{25}{}^b$	2	0.8	0.9	2.5
$J_{26}{}^b$	0.4			
$J_{45}{}^b$	2.7	6	6	2.4
$J_{46}{}^b$	0.4		0.5	0.8
$J_{56}{}^b$	10.3	4	2.3	4.8

[a] Chemical shifts are given in ppm. [b] Coupling constants are given in Hz with a digital resolution of about 0.2 Hz. [c] Signal partially obscured.

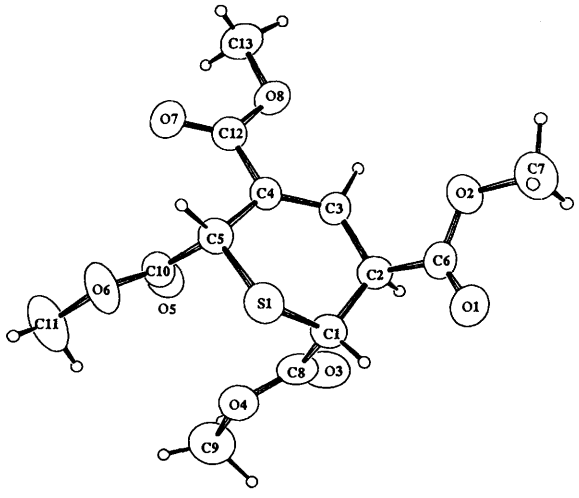

Fig. 3 ORTEP[33] structure of compound **4c**

X-Ray structure analysis

5,6-Dihydro-2*H*-thiopyran obtained by electrochemical reduction in acidic media was crystallized by slow evaporation of a tetrahydrofuran (THF) solution. This molecule corresponds to the **4c** diastereoisomer and the ring adopts a half-chair conformation with the sulfur atom above the ring plane (Fig. 3).

Molecular modelling

Several semi-empirical methods (MNDO, PM3 and AM1) and one molecular mechanics force-field (TRIPOS) have been tested by comparing the energy minimized geometry with the crystal structure conformation. The correlation was evaluated by calculating the root mean square (rms) between all heavy atoms of theoretical against experimental conformations. The TRIPOS force-field (see Experimental section) gives a much better agreement (rms = 0.31 Å) than the MNDO (rms = 1.06 Å), PM3 (rms = 0.64 Å) or AM1 (rms = 0.86 Å) hamiltonians. This force-field was therefore retained for modelling the different diastereoisomers. The 5,6-dihydro-2*H*-thiopyran molecule was constructed with all possible combinations of (*R*) and (*S*) isomers at the three chiral carbons (C-2, C-5 and C-6). For the eight diastereoisomers, two half-chair and two boat conformations have to be considered, leading therefore to 32 starting conformers. However, since mirror images could not be distinguished in these type of calculations, only half of them (*i.e.* one half-chair and one boat conformation) have been built. The geometry of these 16 conformations was fully optimized. It appears that none of the boat shapes corresponds to a stable conformation. Their starting energy was very high and their geometry converged to half-chair shape during the energy minimization. As for the half-chair conformations, they could be optimized and yield conformations with similar energy levels. Their energies are listed in Table 3. Fig. 4 displays the optimized conformations of the half-chairs and their geometrical characteristics.

Discussion

Conformations of the 2,3,5,6-tetramethoxycarbonyl-5,6-dihydro-2*H*-thiopyrans

Many conformations studies deduced from ^{1}H NMR spectra lead to the conclusion that cyclohexene,[15,16] dihydropyrans[17,18] and dihydrothiopyrans[10,19,20] adopt predominantly the half-chair conformation in solution. However, some substituted 3,4-dihydrothiopyran rings appear to prefer a boat form.[21] In our case, the two considered conformations are illustrated in Scheme 3. For each boat and half chair conformation, the

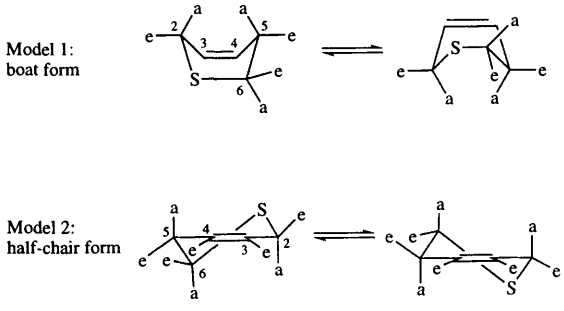

Scheme 3

dihedral angles between 5-H–C-5–C-6–6-H and 4-H–C-4–C-5–5-H were compared with the calculated angles from the observed vicinal coupling constants, using the well known Karplus equation. This correlation between coupling constants and dihedral angles is established for $^3J_{5\text{-H},6\text{-H}}$ and $^3J_{4\text{-H},5\text{-H}}$ from the fragments H–Csp^3–Csp^3–H[22-24] and H–Csp^2–Csp^3–H,[25,26] respectively.

In the case of a boat form, the C-5 and C-6 substituents adopt a staggered form and suggest two values for $^3J_{5\text{-H},6\text{-H}}$. Experimentally, the observed values from ^{1}H NMR data indicate three vicinal couplings in agreement with the 5-H–C-5–C-6–6-H dihedral angles compatible with the half-boat form. Moreover, the measured values for $^3J_{4\text{-H},5\text{-H}}$ (2.5 and 6 Hz) are in agreement with the half-chair conformation of 5,6-dihydro-2*H*-thiopyrans in solution (model 2 in Scheme 3).

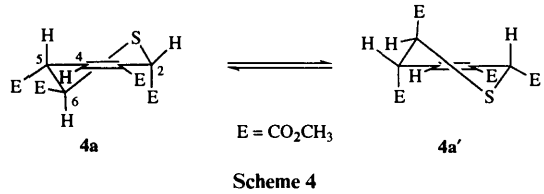

Scheme 4

Upon examination of the boat conformation it would be predicted that the coupling constant for $^3J_{4\text{-H},5\text{-H}}$ could not be less than 5 Hz.[10,19,20]

Identification of diastereoisomers

To identify the relative configuration of the diastereoisomers, it would be necessary to determine the axial or equatorial position of the ring protons. The possible correlation between

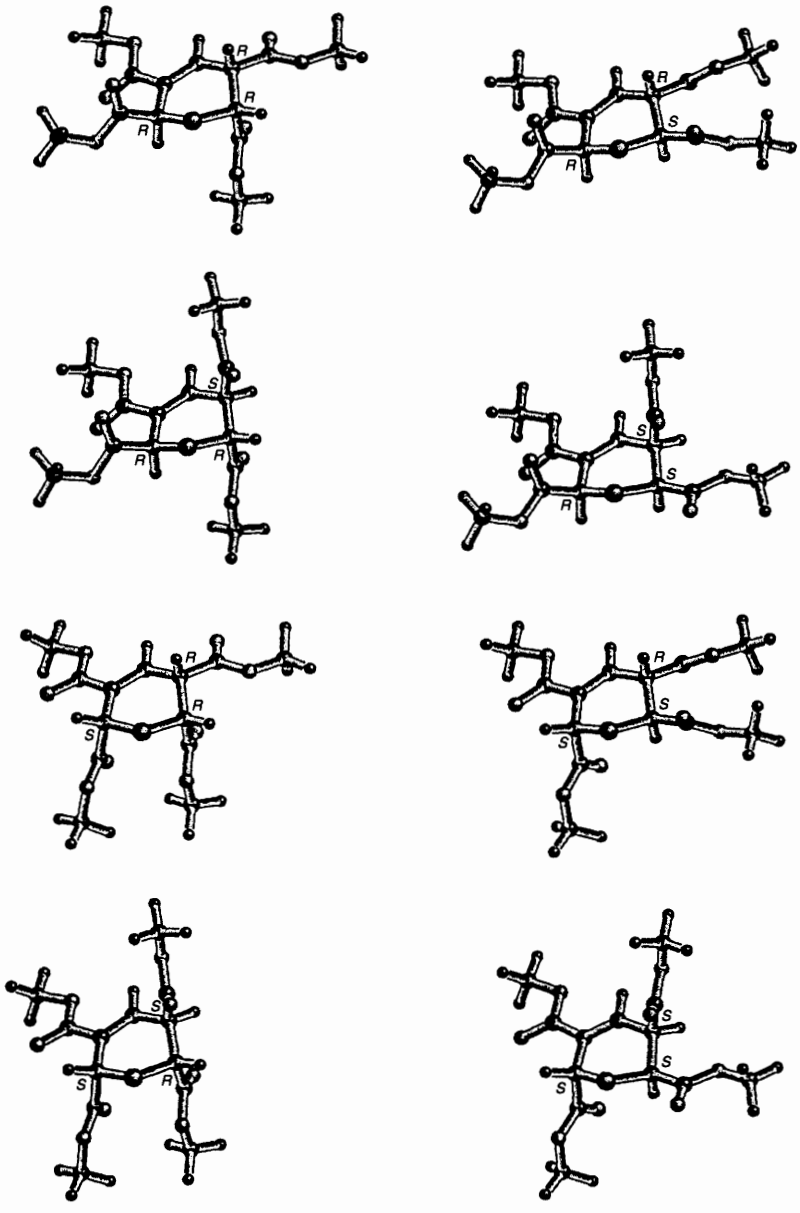

Fig. 4 Molecular modelling of the half-chair conformations

Table 3 Final energy of the optimized conformations[a]

Conformation	*RRR*	*RRS*	*RSR*	*RSS*	*SRR*	*SRS*	*SSR*	*SSS*
Final energy kcal mol^{-1}	−8.8	−10.4	−12	−6.6	−5	−11.2	−13.9	−13.1

[a] 1 cal = 4.184 J.

the vicinal ^3J,[22-26] allylic ^4J[27] over four σ-bonds[28] and homoallylic ^5J[29] coupling constants was then used. This approach is summarized in Table 4.

The structural determinations for each diastereoisomer **4a–d** indicate the following.

(*i*) In the case of compound **4a**, a *trans*-diaxial position for the 5-H and 6-H protons should predict a theoretical coupling constant J 13.[29] The lowest value reported in Table 2 for **4a** ($^3J_{5\text{-H},6\text{-H}}$ 10.3) could result from a low participation of the minor conformation **4a** in equilibrum with **4a′** inducing an average of the coupling constants[26] (Scheme 4).

(*ii*) On the other hand, the excellent correlation between the dihedral angles and the coupling constants enables assignment of conformations described in Scheme 5 to the diastereoisomers **4b** and **4c**. The stereochemistry of the 5,6-dihydro-2*H*-thiopyran **4c** was confirmed by the X-ray analysis reported here. In the solid state, the half-chair conformation is observed with the H-2, H-5 and H-6 protons in an equatorial position (Fig. 3). These results are in agreement with the ^{1}H NMR analysis in solution concerning the relative stereochemistry of compound **4c**.

(*iii*) In the case of compound **4d**, the correlation between the dihedral angles and the allylic coupling constant $^4J_{2\text{-H},4\text{-H}}$ 1.9 appears to be less obvious. As a result, the value of this coupling constant compared with those observed for the other diastereoisomers seems to be large for an equatorial proton.

Table 4 Coupling constants and their corresponding dihedral angles

Proton	Coupling constants	Dihedral angles
2-H	$^4J_{2\text{-H},4\text{-H}}$	2-H–C-2–C-3=C-4 and C-2–C-3=C-4–4-H
	$^5J_{2\text{-H},5\text{-H}}$	2-H–C-2–C-3=C-4 and C-3=C-4–C-5–5-H
5-H	$^3J_{4\text{-H},5\text{-H}}$	4-H–C-4–C-5–5-H
	$^5J_{2\text{-H},5\text{-H}}$	2-H–C-2–C-3=C-4 and C-3=C-4–C-5–5-H
6-H	$^4J_{4\text{-H},6\text{-H}}$	4-H–C-4–C-5–C-6 and C-4–C-5–C-6–6-H
	$^3J_{5\text{-H},6\text{-H}}$	5-H–C-5–C-6–6-H

Table 5 Percentages of 5,6-dihydro-2*H*-thiopyran diastereoisomers

5,6-Dihydro-2*H*-thiopyran diastereoisomers	After electrolysis in an acidic medium	After electrolysis in a basic medium	Thermodynamic equilibrium
4a	6	32.5	32.5
4b	27	20	19
4c	43	32	30.5
4d	24	15.5	18

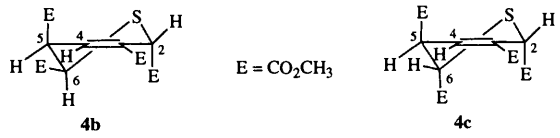

4b **4c**

Scheme 5

However, we can rule out an axial position for 2-H, which should correspond to a conformer of the previously described compound **4b**. Moreover, this assumption should suggest a theoretical coupling constant $^4J_{2\text{-H},4\text{-H}}$, but in fact for **4d** a small proportion of conformation **4d'** resulting from a ring-inversion process may be considered (Scheme 6). The presence of a

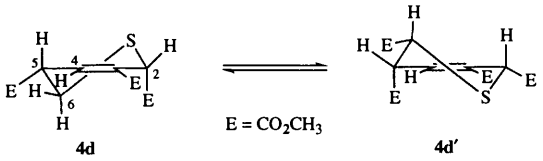

4d **4d'**

Scheme 6

slightly distorted conformation for **4d** owing to the presence of the three methoxycarbonyl substituents on the same side of the ring cannot be excluded.

Quantitative determination of the diastereoisomers

The ratio of the four diastereoisomers **4a–d** depends on the experimental conditions. Kinetic control was observed in acidic conditions. Thermodynamic equilibrium was established by electrolysis under the same acidic conditions and storage overnight under basic conditions. The quantitative determinations were carried out by ^{1}H NMR spectroscopy and are given in Table 5.

The results summarized in Table 5 clearly demonstrate that thermodynamic equilibrium takes place in basic media. In acidic media, the percentage of stereoisomers **4c** and **4d** is clearly higher than in basic media. For these two compounds the hydrogen atoms linked to carbons 2 and 6 are in the *cis* orientation. This observation suggests that under acidic conditions, protonation of carbanionic intermediates occurs from the electrode side, but it is rather speculative to go further in such a discussion without other information. The latter should be obtained from electroreduction of triactived thiopyrans which is now in progress.

Chemical reduction

Chemical reduction with zinc and acetic acid was also carried out. This method has been frequently used for the reduction of C=C double bonds.[30] In this procedure, the result is less selective, because of the formation of the dimer compound **5** during the reduction process as described in Scheme 7. The percentage of the four diastereoisomers resulting from this method is the following: **4a**—17%, **4b**—28%, **4c**—20% and **4d**—35%.

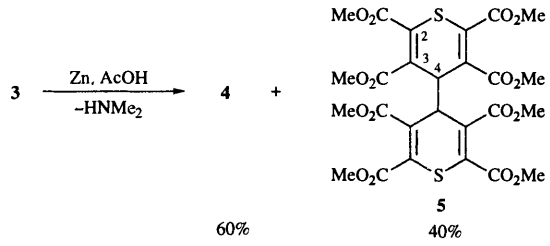

Scheme 7

Experimental

General procedures

^{1}H NMR spectra were recorded on an AM 300 WB (Bruker) instrument. ^{13}C NMR spectra were obtained at 75 MHz. Chemical shifts are given in ppm using $CDCl_3$ and C_6D_6 as solvents and $SiMe_4$ as the internal reference, and coupling constants in Hz. Complete assignments were established by the selective ^{1}H homo- and hetero-decoupling techniques. EIMS were determined on a Varian MAT 311 Spectrometer (inversed Nier-Johnson geometry) at 70 eV. ESIMS was done on a VG Analytical ZABspec TOF spectrometer (EBE TOF geometry) using water–acetonitrile as solvent (1:1). Infrared spectra were recorded on a Nicolet 205 FTIR spectrophotometer for samples in potassium bromide powder. Chromatography was carried out on silica gel columns (Merck 70–230 mesh ASTMS) with ethyl acetate and light petroleum (bp 35–60 °C) as eluents. Melting points were determined using a Kofler apparatus. Elemental analysis was performed by the Microanalyse Service of CNRS (Vernaison, France).

Electrochemistry

Polarograms were recorded at a dropping mercury electrode (dropping time $\tau = 2$ s) with a three electrode PAR 362 potentiostat coupled with a XY Kipp & Zonen recorder. The substrate concentration was 10^{-3} mol l^{-1} in a mixture of aqueous supporting electrolyte and ethanol (1:1). The composition of the three supporting electrolyte was: sulfuric acid (0.5 mol l^{-1}); acetate buffer (CH_3COOH, 0.5 mol l^{-1} and $NaCH_3CO_2$, 0.5 mol l^{-1}); ammoniacal buffer (NH_4Cl, 0.5 mol l^{-1} and NH_3, 0.5 mol l^{-1}).

Preparative electrolysis was carried out at a mercury pool electrode in the cell described by Moinet and Peltier.[31] The working potential was imposed by a Tacussel PRT potentiostat while the reference electrode was a saturated calomel electrode (SCE). The amount of electricity was measured with a Tacussel IG5 coulometer. For a typical run, 10^{-2} to 10^{-3} mol of the substrate was dissolved in 180 ml of the catholyte (aqueous supporting electrolyte and ethanol 1:2). Electrolyte was then performed under a continuous nitrogen flow. An auxiliary polarographic device was used: polarograms were recorded during electrolysis in order to control advancement of the reduction or to detect evolution of the reduced compound. After complete electrolysis, the solution was worked up by decanting the mercury, removal of ethanol under reduced pressure and extraction with dichloromethane. The organic layer was then worked up as follows. (*i*) Purification for characterization: after neutralization of the solution, the organic layer was dried over magnesium sulfate and purified by chromatography on a silica gel column (eluent: 60:40 ethyl acetate–light petroleum). (*ii*) Extraction for quantitative determination: after drying over magnesium sulfate, the solvent was evaporated.

4-Dimethylamino-2-phenyl-5,6-dimethoxycarbonyl-4*H*-1,3-thiazine

Preparation and physicochemical characteristics have been previously given in the literature.[14]

Preparation of the 3-dialkylaminoprop-2-ene-1-thiones 2

Method A. A solution of 4*H*-1,3-thiazine (3 mmol) was heated in dichloromethane (20 ml) at reflux. The progress of the thermolysis was followed by TLC. The resulting thioamide

vinylogue **2** was purified on a silica gel column (eluent: 60:40 light petroleum–ethyl acetate) and crystallized from ethyl acetate (yield: 83%).

Method B. The N^1-thioacylformamidine **1** (5 mmol) was added at room temperature to DMAD (5 mmol) in 15 ml of dichloromethane. The reaction mixture was stirred continuously at room temperature for 2 h and the solution then progressively heated to 40 °C. The rest of the procedure was identical to the previous method. Physicochemical characteristics are in agreement with the literature.[14]

Preparation of the 4-dimethylamino-2,3,5,6-tetramethoxycarbonyl-4*H*-thiopyran 3

A mixture of the thioamide vinylogue (4.2 mmol) and DMAD (4.5 mmol) in dichloromethane (30 ml) was heated at reflux and the reaction was followed by TLC. After evaporation of the solvent, the reaction product was purified on a silica gel column (eluent: 50:50 light petroleum–ethyl acetate). Physicochemical characteristics agree with the literature.[14]

General analysis of the diastereoisomers 4a–d

The diastereoisomers **4a–d** showed the following (74% in acidic medium 82% in basic conditions): yellow oil; ν_{max}/cm^{-1} 1738, 1729 and 1722 (CO) (Found: C, 47.11; H, 4.96; S, 9.63. $C_{13}H_{16}O_8S$ requires C, 46.98; H, 4.85; S, 9.65%); *m/z* (EI) 332 ($M^{+\cdot}$, 5%); 300 (33, M − MeOH); 268 (35, M − 2 MeOH); 241 (27, M − MeOH − CO_2Me); 240 (11, M − 2 MeOH − CO); 213 (100 M − 2 CO_2Me − H)]; *m/z* (HREI) Found: $M^{+\cdot}$, 332.0549. $C_{13}H_{16}O_8S$ requires M, 332.0566; Found: $M^{+\cdot}$ − MeOH, 300.0319. $C_{12}H_{12}O_7S$ requires M, 300.0304]; ^1H NMR data are given in Table 2.

^{13}C NMR data of 4a–d. 4a showed $\delta_C(CDCl_3)$: 39.1 (dq, ^1J 149, ^3J and ^2J 5, C-6), 39.8 (dd, ^1J 144, ^3J 9, C-2), 46.1 (br d, ^1J 132, ^2J 4, C-5), 52.5, 53, 53.1, 53.2 (CO_2CH_3), 127.2, (st, ^3J and ^2J 7, C-3), 139.2, (ddd, ^1J 166, ^3J 9, ^3J 5, C-4), 165.1 (3-CO_2CH_3), 169.8, 170.1, 170.4 (Csp^3-CO_2CH_3). **4b**: $\delta_C(CDCl_3)$: 39.9 (dd, ^1J 144, ^3J 8, C-2), 41 (dq, ^1J 145, ^3J and ^2J 5, C-6), 43.8 (dd, ^1J 131, ^2J 3, C-5), 52.8, 52.9, 53, 53.1 (CO_2CH_3), 128 (br s, ^3J 7, ^2J 5, C-3), 138.9 (ddd, ^1J 168, ^3J 9 and 5, C-4), 165.2 (3-CO_2CH_3), 168.7, 169.3, 171 (Csp^3-CO_2CH_3). **4c**: $\delta_C(CDCl_3)$: 37.4 (ddd, ^1J 142, ^3J 8, ^2J 5, C-2), 38.9 (dq, ^1J 139, ^3J 9, ^3J and ^2J 5, C-6), 42.2 (dm, ^1J 129, ^2J 7 and 4, C-5), 52.4, 52.5, 53.1, 53.2 (CO_2CH_3), 126.8 (sm, ^2J 3, ^3J 5, C-3), 137.1 (m, ^1J 167, ^3J 9, ^2J and ^3J 5, C-4), 165.3 (3-CO_2CH_3), 169.7, 170, 170.3 (Csp^3-CO_2CH_3). **4d**: $\delta_C(CDCl_3)$: 37.7 (dt, ^1J 142, ^3J 7, ^3J 6, C-2), 38.4 (dq, ^1J 142, ^3J and ^2J 5, C-6), 44.1 (dd, ^1J 126, ^2J 5, C-5), 52.4, 52.5, 53.1, 53.2 (CO_2CH_3), 125.3 (br s, ^3J 7, ^2J 5, C-3), 137.9 (dq, ^1J 168, ^3J 9, ^3J and ^2J 5, C-4), 165.5 (3-CO_2CH_3), 169.6, 169.1, 170.5 (Csp^3-CO_2CH_3).

General analysis of dimer 5

Compound **5** was obtained as a yellow powder, mp 225–227 °C; ν_{max}/cm^{-1} 1735 and 1718 (CO); *m/z* (HREI) Found: $M^{+\cdot}$, 329.0331. $C_{13}H_{13}O_8S$ requires M, 329.0334]; *m/z* (HRESI) Found: $M + Na^+$, 681.0568. $C_{26}H_{26}O_{16}S_2Na$ requires M, 681.056; $\delta_H(CDCl_3)$ 4.92 (1 H, s, 4-H), 3.78 (6 H, s, 2-CO_2CH_3), 3.86 (6 H, s, 3-CO_2CH_3); $\delta_C(CDCl_3)$ 36.4 (dd, ^1J 143, ^2J 6, C-4); 53.1 (t, ^1J 148, 3-CO_2CH_3), 53.5 (t, ^1J 148, 2-CO_2CH_3), 125.2 (C-3), 138.2 (C-2), 163.4 (m, ^3J 4 and 2, 3-CO_2CH_3), 164.2 (q, ^3J 4, 2-CO_2CH_3).

X-Ray analysis of compound 4c

$C_{13}H_{16}O_8S$: $M_r = 488.6$, monoclinic, $P2_1/n$, $a = 9.210(2)$, $b = 10.322(9)$, $c = 16.194(9)$ Å, $\beta = 98.14(2)°$, $V = 1524(1)$ Å^3, $Z = 4$, $D_c = 1.45$ Mg m^{-3}, λ (Mo-Kα) = 0.709 26 Å, $\mu = 2.38$ cm^{-1}, $F(000) = 696$, $T = 294$ K, final $R = 0.072$ for 1593 observations. The sample (0.31 × 0.35 × 0.35 mm) was studied on an Enraf-Nonius CAD 4 automatic diffractometer with graphite monochromatized Mo-Kα radiation. The cell parameters were obtained by fitting a set of 25 high reflections. The data collection ($2\theta_{max} = 50°$, scan $\omega/2\theta = 1$, $t_{max} = 60$ s, range *hkl*: *h* 0, 10; *k* 0, 12; *l* − 19,19), without appreciable intensity decay (0.4%) gave 3038 reflections of which 1593 ($R_{int} = 0.015$) had $I > 3\sigma(I)$ and were used subsequently. After Lorenz and polarization corrections the structure was solved by direct methods which revealed most of the atoms of the molecule. The remaining non-hydrogen atoms of the structure were found after successive scale factor refinements and Fourier differences. After isotropic ($R = 0.11$), then anisotropic refinement ($R = 0.080$), the hydrogen atoms were found with a Fourier difference (between 0.67 and 0.26 e Å^{-3}). The structure was refined on *F* by the full-matrix least-square techniques {*x*, *y*, *z*, β_{ij} for S, O and C atoms and *x*, *y*, *z* for H atoms; 248 variables and 4895 observations; $w = 1/\sigma(F_o)^2 = [\sigma^2(I) + (0.04F_o^2)^2]^{-1/2}\}$ to $R = 0.074$, $R_w = 0.072$ and $S_w = 2.82$ (residual $\Delta\rho \leq 0.27$ e Å^{-3}). Atomic scattering factors are from International Tables for X-ray Crystallography.[32] All the calculations were performed on a Digital Micro VAX 3100 computer with the MOLEN package.[33]

Atomic coordinates, bond lengths and angles, and thermal parameters have been deposited at the Cambridge Crystallographic Data Centre (CCDC). For details of the deposition scheme, see 'Instructions for Authors', *J. Chem. Soc., Perkin Trans. 2*, 1996, Issue 1. Any request to the CCDC for this material should quote the full literature citation and the reference number 188/33.

Molecular modelling

Semi-empirical calculations have been performed using the MOPAC package.[35] Molecular mechanics calculations were done with the TRIPOS force-field[36] of the SYBYL package.[37] AM1 charges were used for the calculations of the electrostatic contribution. Conjugate gradient method was used for energy minimization. The termination option was set to a value of 0.01 for the rms gradient.

References

1 B. Bujoli, M. Jubault, J. C. Roze and A. Tallec, *Tetrahedron*, 1987, **43**, 2709.
2 A. Abouelfida, J. P. Pradère, M. Jubault and A. Tallec, *Can. J. Chem.*, 1992, **70**, 14.
3 A. Imberty, F. Tonnard, A. Abouelfida, J. P. Pradère, M. Jubault and A. Tallec, *Sulfur Lett.*, 1993, **16**, 103.
4 G. Casy and R. J. K. Taylor, *Tetrahedron*, 1989, **45**, 455.
5 J. P. Pradère, G. Bouet and H. Quiniou, *Tetrahedron Lett.*, 1972, **33**, 3471.
6 T. Karakasa and S. Motoki, *J. Org. Chem.*, 1978, **43**, 4147; 1979, **44**, 4151.
7 K. Kanakarajan and H. Meier, *J. Org. Chem.*, 1983, **48**, 881.
8 H. Quiniou, *Phosphorus and Sulfur*, 1981, **10**, 1.
9 K. R. Lawson, A. Singleton and G. H. Whitman, *J. Chem. Soc., Perkin Trans. 1*, 1984, p. 859; 1984, p. 865.
10 I. T. Barnish, C. W. G. Fishwick, D. R. Hill and C. Szantay Jr, *Tetrahedron*, 1989, **45**, 6771.
11 J. P. Pradère, Y. T. N'Guessan, H. Quiniou and F. Tonnard, *Tetrahedron*, 1975, **31**, 3059.
12 D. L. Boger and S. M. Weinreb, *Hetero–Diels–Alder Methodology in Organic Synthesis*, Acadamic, San Diego, 1987, pp. 220–223.
13 J. Kuthan, P. Sebek and S. Böhm, *Advances in Heterocyclic Chemistry*, Academic, San Diego, 1994, vol. 59, p. 213.
14 J. P. Pradère, F. Tonnard, A. Abouelfida, C. Cellerin, M. Andriamanamihaja, B. Jousseaume, L. Toupet and P. Guenot, *Bull. Soc. Chim. Fr.*, 1993, **130**, 610.
15 N. L. Allinger and J. J. Sprague, *J. Am. Chem. Soc.*, 1972, **94**, 5734.
16 R. P. Johnson and K. J. Dirico, *J. Org. Chem.*, 1995, **60**, 1074.
17 O. Achmatowicz, Jr., M. Chmielewski, J. Jurczak, L. Kozerski and A. Zamojski, *Org. Magn. Reson.*, 1972, **4**, 537.
18 A. Deboer, *Org. Magn. Reson.*, 1973, **5**, 7.
19 J. P. Pradère and G. Hadjukovic, *C. R. Acad. Sci. Paris*, 1978, **286(C)**, 553.
20 P. M. Henrichs and C. H. Chen, *J. Org. Chem.*, 1979, **44**, 3591.
21 J. S. A. Brunskill, A. De and D. F. Ewing, *Org. Magn. Reson.*, 1979, **12**, 257.
22 M. J. Karplus, *J. Am. Chem. Soc.*, 1963, **85**, 2870.

23 C. A. G. Haasnoot, F. A. A. M. De Leeuw and C. Altona, *Tetrahedron*, 1980, **36**, 2783.
24 M. Barfield and W. B. Smith, *J. Am. Chem. Soc.*, 1992, **114**, 1574.
25 E. W. Garbisch, *J. Am. Chem. Soc.*, 1964, **86**, 5561.
26 S. Sternhell, *Q. Rev. Chem. Soc.*, 1969, **23**, 236.
27 M. Barfield and B. Chakrabarti, *Chem. Rev.*, 1969, **69**, 757.
28 M. Barfield, M. D. Alison, C. J. Fallick, R. J. Spear, S. Sternhell and P. W. Westerman, *J. Am. Chem. Soc.*, 1975, **97**, 1482.
29 M. Barfield and S. Sternhell, *J. Am. Chem. Soc.*, 1972, **94**, 1905.
30 J. McKenna, J. K. Norymberski and R. D. Stubbs, *J. Chem. Soc.*, 1959, 2502.
31 C. Moinet and D. Peltier, *Bull. Soc. Chim. Fr.*, 1969, 690.
32 *International Tables for X-ray Crystallography*, Birmingham, Kynoch Press, present distributor D. Reidel, Dordrecht, 1974, vol. IV.
33 C. K. Fair, *MOLEN. An Interactive Intelligent System for Crystal Structure Analysis*, Enraf-Nonius, Delft, The Netherlands, 1990.
34 C. K. Johnson, ORTEP, Report ORNL—3794. Oak Ridge National Laboratory, Tennessee, USA, 1965.
35 M. Clark, R. D. Cramer III and N. Van Opdenbosch *J. Comput. Chem.*, 1989, **10**, 982.
36 MOPAC, V6.0, QCPE Program No. 455.
37 SYBYL, V6.0, Tripos Associates, 1699, S. Hanley Road, Suite 303, St Louis MO63144, USA.

Paper 6/04128K
Received 12*th June* 1996
Accepted 6*th August* 1996